

Accepted Manuscript

Design, Synthesis and Biological Evaluation of 2,4-Disubstituted Oxazole Derivatives as Potential PDE4 Inhibitors

Ya-Sheng Li, De-Kun Hu, Dong-Sheng Zhao, Xing-Yu Liu, Hong-Wei Jin, Gao-Peng Song, Zi-Ning Cui, Lian-Hui Zhang

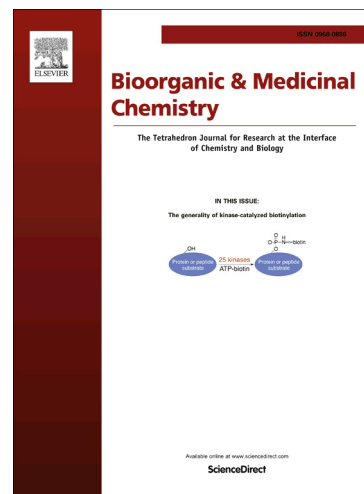
PII: S0968-0896(16)31240-8
DOI: <http://dx.doi.org/10.1016/j.bmc.2017.01.047>
Reference: BMC 13526

To appear in: *Bioorganic & Medicinal Chemistry*

Received Date: 19 November 2016
Accepted Date: 31 January 2017

Please cite this article as: Li, Y-S., Hu, D-K., Zhao, D-S., Liu, X-Y., Jin, H-W., Song, G-P., Cui, Z-N., Zhang, L-H., Design, Synthesis and Biological Evaluation of 2,4-Disubstituted Oxazole Derivatives as Potential PDE4 Inhibitors, *Bioorganic & Medicinal Chemistry* (2017), doi: <http://dx.doi.org/10.1016/j.bmc.2017.01.047>

This is a PDF file of an unedited manuscript that has been accepted for publication. As a service to our customers we are providing this early version of the manuscript. The manuscript will undergo copyediting, typesetting, and review of the resulting proof before it is published in its final form. Please note that during the production process errors may be discovered which could affect the content, and all legal disclaimers that apply to the journal pertain.



Design, Synthesis and Biological Evaluation of 2,4-Disubstituted Oxazole Derivatives as Potential PDE4 Inhibitors

Ya-Sheng Li ^{a,#}, De-Kun Hu ^{a,#}, Dong-Sheng Zhao ^{d,#}, Xing-Yu Liu ^a,
Hong-Wei Jin ^e, Gao-Peng Song ^{c,*}, Zi-Ning Cui ^{a,b,*}, Lian-Hui Zhang ^a

^a State Key Laboratory for Conservation and Utilization of Subtropical Agro-bioresources, Integrative Microbiology Research Centre, Guangdong Province Key Laboratory of Microbial Signals and Disease Control, South China Agricultural University, Guangzhou 510642, China

^b Key Laboratory of Green Pesticide and Agricultural Bioengineering, Ministry of Education, Guizhou University, Guiyang 550025, China

^c College of Materials and Energy, South China Agricultural University, Guangzhou 510642, China;

^d Department of Pharmacy, Quanzhou Medical College, Quanzhou 362100, China

^e State Key Laboratory of Natural and Biomimetic Drugs, School of Pharmaceutical Sciences, Peking University, Beijing 100191, China

[#]Both authors contributed equally to this paper.

*Corresponding author. Tel.: +86-20-85288229; Fax: +86-20-85288229

E-mail address: ziningcui@scau.edu.cn (Z. C.), vinsin1021@126.com (G. S.)

Abstract: In this study, a series of pyrazole derivatives containing 4-phenyl-2-oxazole moiety were designed and synthesized in a concise way, some of which exhibited considerable inhibitory activity against PDE4B and blockade of LPS-induced TNF- α release. Compound **4c** displayed the strongest inhibition activity ($IC_{50} = 1.6 \pm 0.4 \mu M$) and good selectivity against PDE4B. Meanwhile, compound **4c** showed good *in vivo* activity in animal models of asthma/COPD and sepsis induced by LPS. The primary structure–activity relationship study showed the 3,5-dimethylpyrazole residue was essential for the bioactivity, and the substituted group R_1 at the benzene ring also affected the activity. Docking results showed that compound **4c** played a key role to form integral hydrogen bonds and a π - π stacking interaction, using hydrazide scaffold (-CO-N-N-) and pyrazole ring respectively, with PDE4B protein. While the rest part of the molecule extended into the catalytic domain to block the access of cAMP and formed the foundation for inhibition of PDE4B. Compound **4c** would be great promise as a lead compound for further study based on the preliminary structure-activity relationship and molecular modeling studies.

Keywords: synthesis; 4-phenyl-2-oxazole; pyrazole derivatives; PDE4 inhibitor; molecular simulation

1. Introduction

Cyclicadenosine monophosphate (cAMP) and cyclicguanosine monophosphate (cGMP), the secondary signal messengers, are involved in the regulation of almost all physiological processes. In airway smooth muscle, inflammatory cells, and immune cells, these second messengers play an important role in the regulation of the function. It is well known that cyclic nucleotide phosphodiesterases (PDEs) include 11 diverse families according to their structures and properties.^{1,2} PDE4 plays a key role in the hydrolysis of cAMP and cGMP, which can selectively catalyze the hydrolysis of a 3'-phosphodiester bond, forming an inactive 5'-monophosphate.^{3,4} Thus, inhibition of PDE4 enzymes can result in increasing cellular levels of cAMP, which contributes to both the relaxation of airway smooth muscle and the prevention of proinflammatory cell activation. Therefore PDE4 inhibitors are considered to be potent anti-inflammatory agents for the treatment of inflammatory related diseases, such as asthma and chronic obstructive pulmonary disease (COPD).⁵⁻⁷

For past few decades, PDE4 inhibitors have been extensively studied as anti-inflammatory drugs since the discovery of rolipram and piclamilast (**Fig. 1**) in the early 1990s.^{8,9} Structurally, rolipram and piclamilast belong to diether derivatives of catechol class, some of which have been evaluated in clinic for the treatment of patients with depression, asthma, COPD, dermatitis, neuroinflammation^{10,11} and rheumatoid arthritis.¹² Further structural optimization demonstrated that the 8-methoxyquinoline-5-carboxamides moiety (such as SCH365351, **Fig. 1**)¹³ had excellent PDE4 inhibitory activity. Molecular simulation studies suggested that the quinoline moiety of SCH365351 could bind to the adenosine recognition site. In our previous work,¹⁴ we reported the compounds possessed 7-(cyclopentyloxy)-6-methoxy 1,2,3,4-tetrahydroisoquinoline (**Fig. 1**) showed potential inhibitory activity against PDE4.

It became important to establish selectivity towards one subtype, e.g., PDE4A and PDE4B for PDE4 inhibitory activity to obtain potent and selective inhibitors with an improved therapeutic index and reduced emetic side effects. Recent studies of selective PDE4 inhibitors declared introduction of some groups, such as a short amide linker ($-\text{CONHCH}_2-$) or a 4-methoxy benzyl group, was helpful to enhance the selectivity over other PDE family members.¹⁵ In addition, a five-membered heterocyclic

oxazole moiety was explored as a possible linker to replace the amide portion, which was found to be a highly versatile linker and the derivatives exhibited significantly potent PDE4 inhibitory activity, suggesting it became a key core of PDE4 inhibitors (**Fig. 1**).¹⁶⁻¹⁸ In our recent study,¹⁹ we reported pyrazole and triazole derivatives containing 5-phenyl-2-furan functionality (**Fig. 1**) exhibited considerable inhibitory activity against PDE4B, the subtype of PDE4. The primary SAR results showed that a five-membered heterocycles including oxazole and furan rings could be a key pharmacophore of PDE4 inhibitors. In this study, pyrazole derivatives containing oxazole moiety as the bioisosteric surrogates of the pyrazole and triazole derivatives were further designed and synthesized (**Fig. 1**) in order to obtain the detailed structure-activity relationship, of which inhibitory activity against PDE4B and blockade of LPS-induced TNF- α release was evaluated. Meanwhile the preliminary structure-activity relationship and docking studies were carried out.

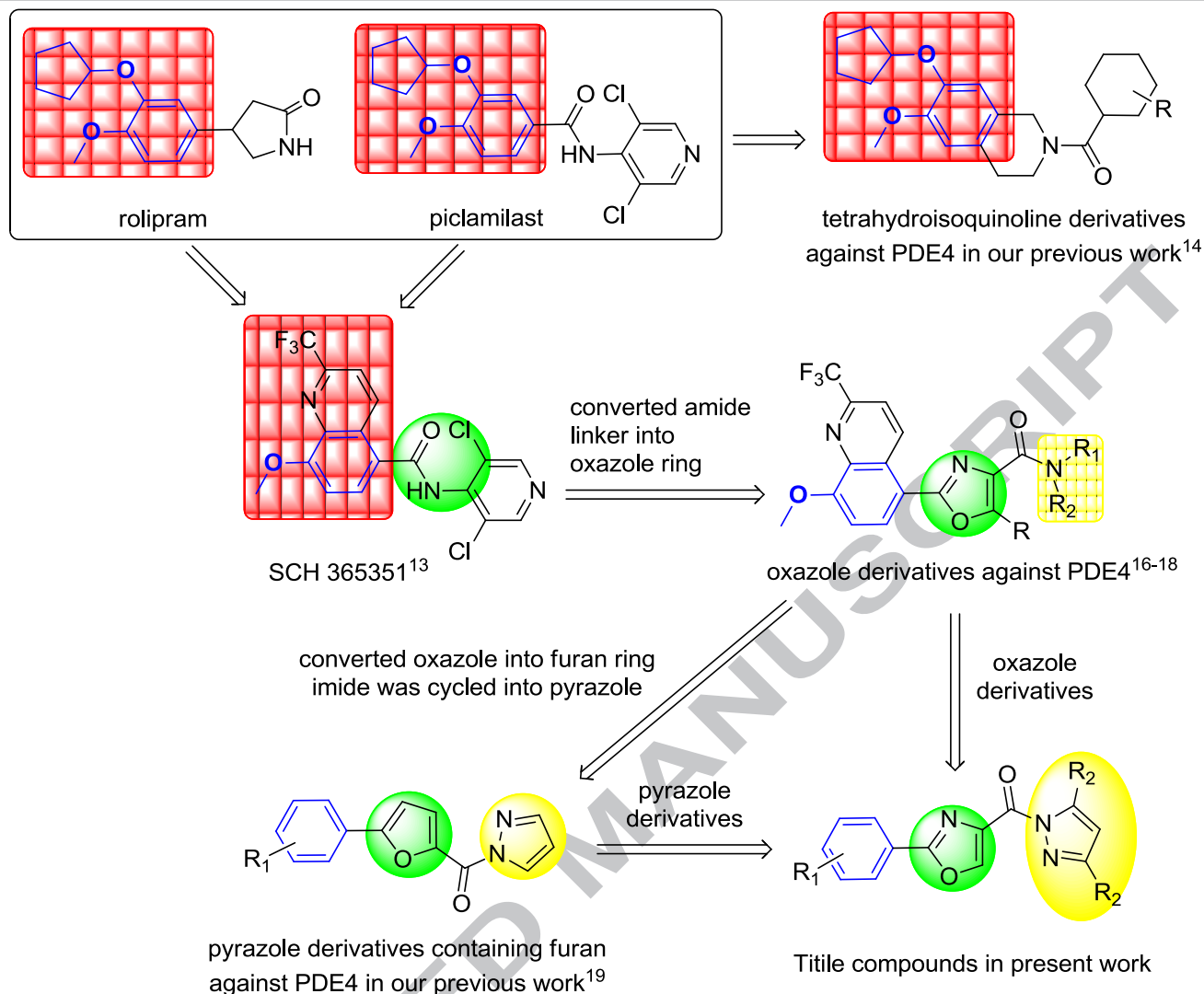


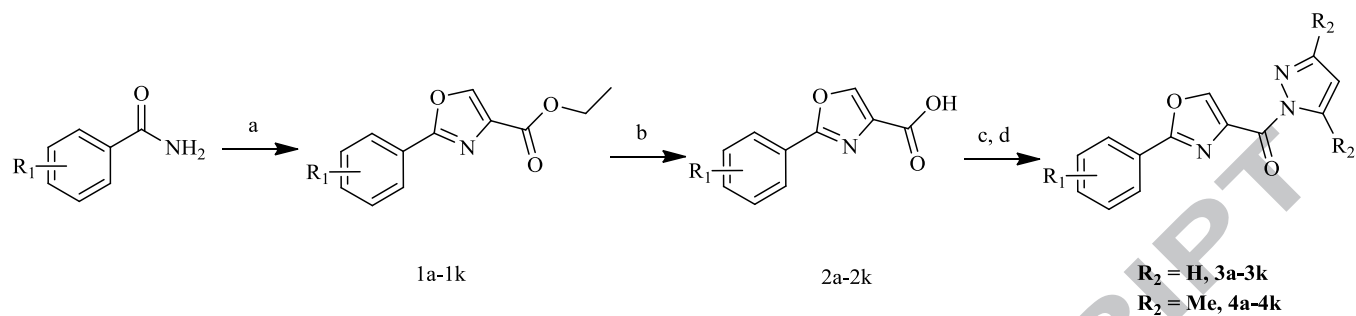
Figure 1. The designed strategy for the title compounds.

2. Results and discussion

2.1. Chemistry

The synthetic route of title compounds **3a-3k** and **4a-4k** was described in **Scheme 1**. The oxazole ethyl esters **1a-1k** were obtained by cyclization of benzoyl amides in the presence of ethyl bromopyruvate under reflux in ethanol for about 5 hours. Then the oxazole ethyl esters were hydrolyzed with 2 M NaOH in water to get the corresponding carboxylic acids **2**, which was reacted with thionyl chloride and pyrazole or 3,5-dimethylpyrazole in anhydrous dichloromethane to obtain the title compounds **3** and **4**. The title compounds have been characterized by melting point, ¹H NMR, ¹³C NMR, mass spectrometry

and elementary analysis. All spectral data were consistent with the assigned structures (the spectra of ^1H NMR and ^{13}C NMR were shown in supplementary materials).



Scheme 1. The synthetic route of the title compounds **3a-3k** and **4a-4k**. Reagents and conditions: (a) ethyl bromopyruvate, ethanol, reflux, 5 h; (b) 2 M NaOH, r.t., 10 h; (c) SOCl_2 , anhydrous toluene, reflux, 4 h; (d) pyrazole or 3,5-dimethylpyrazole, anhydrous dichloromethane, reflux, 4 h, 80-92% in two steps. $\text{R}_1 = \mathbf{3a}$: 4-Cl; $\mathbf{3b}$: 2-OH; $\mathbf{3c}$: 4-OCH₃; $\mathbf{3d}$: 4-CH₃; $\mathbf{3e}$: 3-OCH₃; $\mathbf{3f}$: H; $\mathbf{3g}$: 4-Br; $\mathbf{3h}$: 4-F; $\mathbf{3i}$: 3-OH; $\mathbf{3j}$: 4-OH; $\mathbf{3k}$: 3-F; $\mathbf{4a}$: 4-Cl; $\mathbf{4b}$: 2-OH; $\mathbf{4c}$: 4-OCH₃; $\mathbf{4d}$: 4-CH₃; $\mathbf{4e}$: 3-OCH₃; $\mathbf{4f}$: H; $\mathbf{4g}$: 4-Br; $\mathbf{4h}$: 4-F; $\mathbf{4i}$: 3-OH; $\mathbf{4j}$: 4-OH; $\mathbf{4k}$: 3-F.

2.2. Biological evaluation and SAR studies

In vitro activity for the inhibition of PDE4B and blockade of LPS-induced TNF- α release were listed in **Table 1**. Rolipram was chosen as the positive control. From the results in **Table 1**, it revealed that the activity of title compounds containing 3,5-dimethylpyrazole (series **4**) was better than that of the compounds containing pyrazole (series **3**). For example, the IC₅₀ values of compounds **4c** ($\text{R}_1 = 4\text{-OCH}_3$, $\text{R}_2 = \text{Me}$) and **4d** ($\text{R}_1 = 4\text{-CH}_3$, $\text{R}_2 = \text{Me}$) against PDE4B were 1.6 μM and 6.7 μM respectively, which were better than that of the compounds **3c** ($\text{R}_1 = 4\text{-OCH}_3$, $\text{R}_2 = \text{H}$, IC₅₀ = 3.2 μM) and **3d** ($\text{R}_1 = 4\text{-CH}_3$, $\text{R}_2 = \text{H}$, IC₅₀ = 17.5 μM).

The different activities of compounds **3a-3k** and **4a-4k** with various substitution effects on a benzene ring demonstrated that the modification of the substituted group R_1 at the benzene was significant. Generally, the compounds without any substituted group (**3f** and **4f**, $\text{R}_1 = \text{H}$) gave the poorest activity. Among all the title compounds, **4c** was the most potent inhibitor, and the IC₅₀ value of **4c** was 1.6 μM and 10.3 μM respectively against PDE4B and TNF- α , which showed comparable or better activity than the positive control rolipram (1.8 μM and 18.6 μM) (**Table 1**). Compound **3c**, with the same substituted

group at the same position ($R_1 = 4\text{-OCH}_3$), exhibited considerable IC_{50} values ($3.2 \mu\text{M}$ against PDE4B and $20.8 \mu\text{M}$ against $\text{TNF-}\alpha$) to that of rolipram. Compounds **3e** and **4e**, with the same methoxyl group as **3c** and **4c**, but at the different position, demonstrated lower bioactivities (**3e**: $IC_{50} = 5.9 \mu\text{M}$ against PDE4B and $IC_{50} = 45.8 \mu\text{M}$ against $\text{TNF-}\alpha$; and **4e**: $IC_{50} = 4.5 \mu\text{M}$ against PDE4B and $IC_{50} = 18.7 \mu\text{M}$ against $\text{TNF-}\alpha$). It was suggested that a methoxyl group on a benzene ring displayed good activities against PDE4B, and a methoxyl group at *para*-position of a benzene ring had been proven to be the best bioactivity against PDE4B in our recent study¹⁹ and confirmed to the conclusion of earlier research¹⁴. When R_1 was a hydroxyl group, bioactivity of compounds **3b** ($R_1 = 2\text{-OH}$, $IC_{50} = 85.6 \mu\text{M}$ against PDE4B and $IC_{50} = 205.4 \mu\text{M}$ against $\text{TNF-}\alpha$), **3i** ($R_1 = 3\text{-OH}$, $IC_{50} = 39.7 \mu\text{M}$ against PDE4B and $IC_{50} = 88.4 \mu\text{M}$ against $\text{TNF-}\alpha$), **3j** ($R_1 = 4\text{-OH}$, $IC_{50} = 18.4 \mu\text{M}$ against PDE4B and $IC_{50} = 75.5 \mu\text{M}$ against $\text{TNF-}\alpha$) and **4b** ($R_1 = 2\text{-OH}$, $IC_{50} = 54.8 \mu\text{M}$ against PDE4B and $IC_{50} = 138.7 \mu\text{M}$ against $\text{TNF-}\alpha$), **4i** ($R_1 = 2\text{-OH}$, $IC_{50} = 28.9 \mu\text{M}$ against PDE4B and $IC_{50} = 78.4 \mu\text{M}$ against $\text{TNF-}\alpha$), **4j** ($R_1 = 2\text{-OH}$, $IC_{50} = 15.8 \mu\text{M}$ against PDE4B and $IC_{50} = 66.4 \mu\text{M}$ against $\text{TNF-}\alpha$) with respect to substitution at a benzene ring follows the trend: 4->3->2-. When R_1 was a halogen atom at the *para*-position, activity with respect to substitution follows the trend: 4-Cl (**3a** and **4a**: $IC_{50} = 5.3 \mu\text{M}$ and $4.1 \mu\text{M}$) >4-F (**3h** and **4h**: $IC_{50} = 9.8 \mu\text{M}$ and $8.4 \mu\text{M}$) >4-Br (**3g** and **4g**: $IC_{50} = 58.7 \mu\text{M}$ and $54.8 \mu\text{M}$). It was suggested that the electron-donating group (EDG) and the halogen atom at the *para*-position would be favored to the activities. Preliminary structure-activity relationship study showed that substituent at *para*-position of a benzene ring was a crucial point to the bioactivity and a methoxyl group at *para*-position of a benzene ring revealed the promising lead compound **4c** in this study.

Since inhibition of the subtype PDE4D was associated with the emetic response, therefore we evaluated the selected *in vitro* active compounds **3c** and **4c** for their PDE4B selectivity over PDE4D. The results demonstrated that **3c** and **4c** displayed inhibitory effects on PDE4D with IC_{50} values of $8.4 \mu\text{M}$ and $10.6 \mu\text{M}$ (**Table 1**), indicating their obvious selectivity towards PDE4B ($IC_{50} = 3.2 \mu\text{M}$ and $1.6 \mu\text{M}$).

Table 1. Impact on enzymatic potency (PDE4B) and inhibition of $\text{TNF-}\alpha$ release from human blood mononuclear cells stimulated with lipopolysaccharide ^a

Compd.	R ₁	R ₂	PDE4B		TNF- α		PDE4B		TNF- α
			IC ₅₀ (μ M)	IC ₅₀ (μ M)	Compd.	R ₁	R ₂	IC ₅₀ (μ M)	IC ₅₀ (μ M)
3a	4-Cl	H	5.3 \pm 0.2	40.1 \pm 1.2	4a	4-Cl	Me	4.1 \pm 0.6	27.6 \pm 1.3
3b	2-OH	H	85.6 \pm 2.4	205.4 \pm 5.2	4b	2-OH	Me	54.8 \pm 2.6	138.7 \pm 4.8
3c	4-OCH ₃	H	3.2 \pm 0.2	20.8 \pm 1.1	4c	4-OCH ₃	Me	1.6 \pm 0.4	10.3 \pm 0.9
			(8.4 \pm 0.5) ^b					(10.6 \pm 1.1) ^b	
3d	4-CH ₃	H	17.5 \pm 1.1	72.4 \pm 3.4	4d	4-CH ₃	Me	6.7 \pm 0.3	36.7 \pm 1.5
3e	3-OCH ₃	H	5.9 \pm 0.3	45.8 \pm 1.6	4e	3-OCH ₃	Me	4.5 \pm 0.2	18.7 \pm 1.2
3f	H	H	88.7 \pm 2.9	198.6 \pm 5.2	4f	H	Me	75.8 \pm 3.1	198.8 \pm 5.8
3g	4-Br	H	58.7 \pm 2.4	187.4 \pm 4.8	4g	4-Br	Me	54.8 \pm 2.2	167.8 \pm 5.2
3h	4-F	H	9.8 \pm 0.4	54.8 \pm 2.3	4h	4-F	Me	8.4 \pm 0.4	29.7 \pm 1.4
3i	3-OH	H	39.7 \pm 0.9	88.4 \pm 3.5	4i	3-OH	Me	28.9 \pm 1.1	78.4 \pm 2.0
3j	4-OH	H	18.4 \pm 0.7	75.5 \pm 2.7	4j	4-OH	Me	15.8 \pm 0.6	66.4 \pm 1.9
3k	3-F	H	45.1 \pm 1.4	99.6 \pm 3.1	4k	3-F	Me	40.8 \pm 1.5	83.4 \pm 2.1
	rolipram		1.8 \pm 0.2	18.6 \pm 0.8					
			(3.5 \pm 0.3) ^b						

^a Results are the average of at least three assays. ^b IC₅₀ values against PDE4D

LPS induced sepsis model for the measurement of TNF- α inhibition (in female *Swiss Albino* mice) and neutrophilia inhibition for asthma and COPD (in male *Sprague Dawley* rats) with selected *in vitro* active compounds **3c** and **4c** were performed. The details such as oral dosage and number of animals grouped for the experiments were listed in Table 2. The results showed that compound **4c** demonstrated better inhibitory activity against TNF- α release (42.6%) and LPS induced neutrophilia inhibition (39.1%) than the positive control rolipram (40.8% and 30.9%) and compound **3c** (26.1% and 22.4%).

Table 2. LPS induced TNF- α in SA mice and neutrophil influx in BALF of SD rats

Compd.	R ₂	R ₁	<i>Swiss Albino</i> mice (n = 6)		<i>Sprague Dawley</i> rats (n = 6)	
			Does (mg/kg, po)	TNF- α Inhibition (%)	Does (mg/kg, po)	LPS induced neutrophilia (% inhibition)

3c	H	4-OCH ₃	10	26.1	10	22.4
4c	H	4-OCH ₃	10	42.6	10	39.1
		rolipram	10	40.8	10	30.9

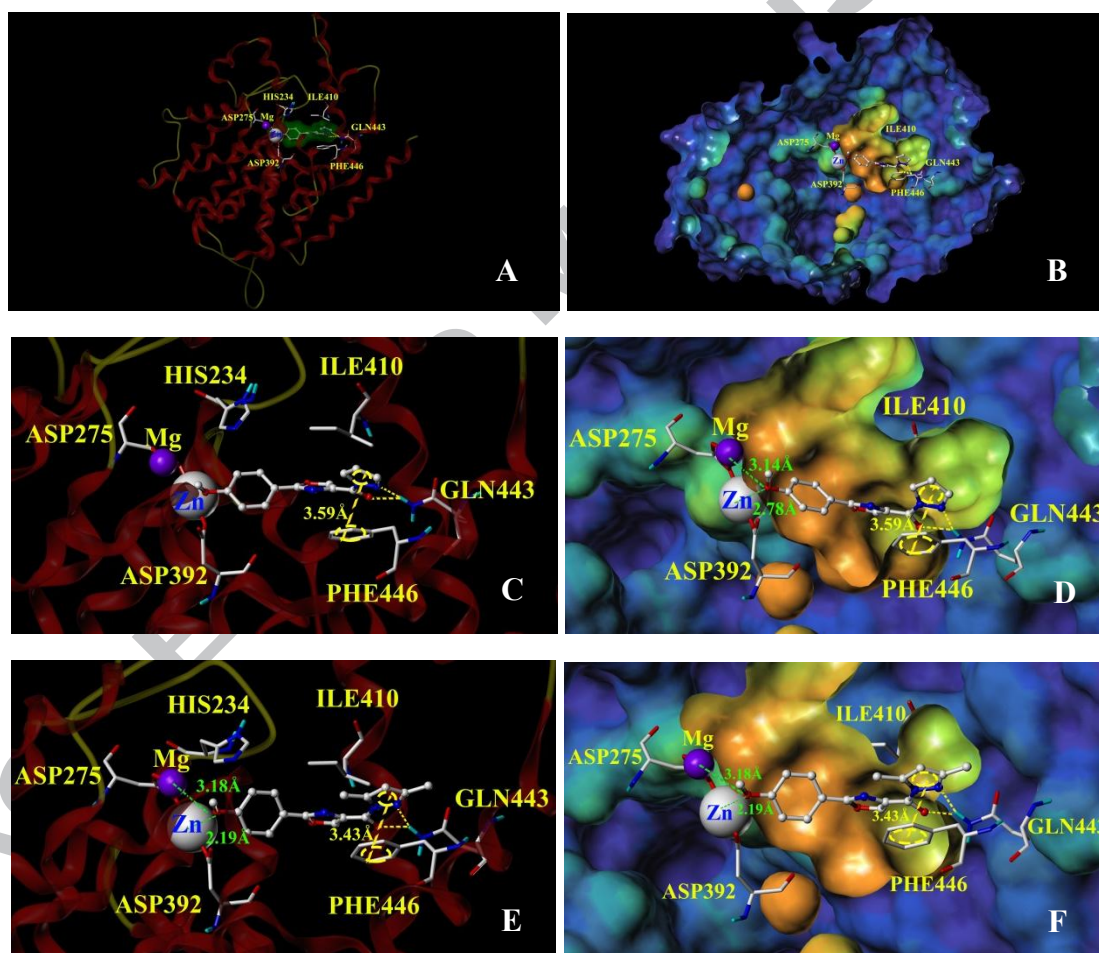
2.3. Docking simulation

Considering the inhibitory activity of title compounds, it was of interest to explore the binding to the PDE4 structure. The bioassay results demonstrated that compounds containing a *para*-methoxy group (**3c** and **4c**) showed the great promise as novel lead compounds for further discovery. Therefore docking simulation of compounds **3c** and **4c** at PDE4B (PDB ID: 1XMY) was conducted using Surflex-Dock in Sybyl 8.0 and the docking contour maps were shown in **Figure 2**.

The docking orientation demonstrated that the five-membered heterocyclic moiety as the pivotal pharmacophore formed integral hydrogen bonds with the conserved glutamine residue (Gln443) (**Fig. 2**) and the heterocyclic ring was evidently positioned between the phenylalanine (Phe446) and isoleucine (Ile410) (**Fig. 2C** and **2E**), which formed the cavity accommodating the hydrophobic moiety of compounds **3c** and **4c**. Particularly, oxygen atom and nitrogen atom of hydrazide moiety (-CO-N-N-) in compounds **3c** and **4c** formed two steady hydrogen bonds with the same hydrogen atom of amide (-CO-NH) in Gln443, which composed a five element ring (**Fig. 2C** and **2E**). In compound **4c**, the oxygen atom of carbonyl group and the nitrogen atom of pyrazole ring interacted with Gln443, which played the same role as the oxygen atoms of methoxy group and cyclopentyloxy group in rolipram respectively (**Fig. 2G** and **2H**). The pyrazole ring in **4c** oriented the similar position with the cyclopentane ring in rolipram. Meanwhile, the pyrazole ring formed a π - π stacking interaction with benzene ring of Phe446 (**Fig. 2C** and **2E**), which enhanced the interaction with PDE4B. Compared with the pyrazole derivative **3c**, the 3,5-dimethylpyrazole moiety of **4c** formed stronger π - π stacking interaction with benzene ring (**3c**: 3.59 Å and **4c**: 3.43 Å, **Fig. 2C** and **2E**) in the phenylalanine (Phe446), and the two methyl groups of **4c** could play a supporting role in the cavity of enzyme, which could also enhance the binding affinity with the enzyme. The remainder of the molecule was displayed to extend into the catalytic domain in close to

both the Zn^{2+} and Mg^{2+} cations (**Fig. 2D** and **2F**), which played a vital role in the catalytic mechanism of cAMP hydrolysis. The *para*-methoxy group (-OMe) formed coordinate bonds with the Zn^{2+} (**3c**: 2.78 Å and **4c**: 2.19 Å, **Fig. 2D** and **2F**) and Mg^{2+} (**3c**: 3.14 Å and **4c**: 3.18 Å, **Fig. 2D** and **2F**) cations. Such orientations and interactions would block the access of cAMP to the catalytic domain and form the foundation for inhibition of PDE4.

In general, compound **4c** exhibited the stronger π - π stacking interaction with phenylalanine (Phe446) and metal coordination with catalytic Zn^{2+} cation than that of compound **3c**. That could give the reason why most title compounds containing 3,5-dimethylpyrazole (series **4**) showed better bioactivity against PDE4B than that of the compounds containing pyrazole (series **3**).



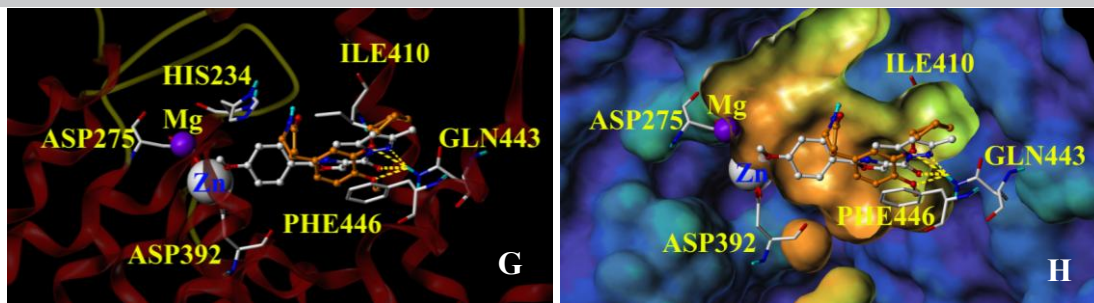


Figure 2. Model of PDE4 and docking of compounds **3c** and **4c**. (A, B) The entire PDE4B structure (N-terminal domain, a catalytic domain and a C-terminal domain) bound to **3c**. (C, D) The catalytic domain bound to **3c**. (E, F) The catalytic domain bound to **4c**. (G, H) The catalytic domain bound to **4c** overlaid with rolipram (orange).

3. Conclusion

In this study, we reported the design, synthesis, and biological evaluation of new phosphodiesterase type 4 inhibitors, containing 2-phenyl-4-oxazole moiety. Their *in vitro* bioactivity against phosphodiesterase type 4 and TNF- α , and *in vivo* activity in animal models of asthma/COPD and sepsis induced by LPS were evaluated. Compound **4c** showed the highest inhibitory activity against PDE4B and blockade of LPS-induced TNF- α release among all the title compounds. A primary structure-activity relationship study showed that the 3,5-dimethylpyrazole residue was favored for the inhibitory activity and substituent at *para*-position of benzene ring in the molecule had an important effect on the inhibitory activity. The docking results suggested that title compounds interacted well with PDE4B protein where a five element ring composing of two intermolecular hydrogen bonds, the π - π stacking interaction, the hydrophobic interaction and the metal coordination in the ligand-receptor complex were vital for the binding affinity. Such efforts were helpful for the further development of novel and effective PDE4 inhibitors.

4. Experimental procedure

4.1. Chemistry

All solvents and reagents were obtained from commercial sources without further purification. ^1H NMR and ^{13}C NMR spectra were recorded on Bruker Avance DRX spectrometer at 600 and 150 MHz.

Chemical shifts are reported as δ values in parts per million (ppm), while tetramethylsilane (TMS) was used as an internal standard. Peak multiplicities are expressed as follows: s, singlet; d, doublet; t, triplet; q, quartet; dd, doublet of doublets; td, triplet of doublets; ddd, doublet of doublet of doublets; brs, broad singlet; m, multiplet. Coupling constants (J values) are given in hertz (Hz). Compounds were dissolved in DMSO- d_6 or in $CDCl_3$. Mass spectra were recorded on a Q-TOF Global mass spectrometer. Elemental analysis was carried out with a Flash EA 1112 elemental analyzer. All the melting points were determined with a Cole-Parmer melting point apparatus while the thermometer was uncorrected. Thin-layer chromatography (TLC) was performed using Merck 60 F254 silica gel plates. Column chromatography was performed using silica gel (200-300 mesh, Qingdao, China) with a linear solvent gradient.

4.1.1. General synthesis of ethyl aryl-1,3-oxazole-4-carboxylates (**1a-1k**).

Amide (1.0 equiv) and ethyl bromopyruvate (1.2 equiv) were dissolved in ethanol and heated to 70 °C for 5 h. The reaction was monitored with TLC until completion. The solvent was evaporated, dried over anhydrous $MgSO_4$. The ethyl ester (**1a-1k**) was purified by flash column chromatography (ethyl acetate/cyclohexane 3:7 (v/v)).

4.1.2. General synthesis of 2-substituted phenyl-4-oxazolecarboxylic acid (**2a-2k**).

The ethyl ester (**1a-1k**) was hydrolyzed by dissolving in EtOH/H₂O, adding 2 M NaOH (5 equiv) and stirring at room temperature for 10 h. Upon completion of the reaction, the solvent was evaporated in vacuum and the reaction mixture was extracted with ethyl acetate. The aqueous layer was acidified with 2 M HCl to pH 2 and the product precipitated. The precipitate was filtered, washed with water and dried to afford the carboxylic acids **2a-2k**.

4.1.3. General synthesis of the title compounds **3** and **4**.

A mixture of 2-substituted phenyl-4-oxazolecarboxylic acid **2** (100 mmol) and thionyl chloride (500 mmol) was refluxed in anhydrous benzene for 4 h. The excess of thionyl chloride and the solvent were distilled off, and the residue was dissolved in anhydrous dichloromethane. The solution of 2-phenyl-4-oxazolecarbonyl chloride in anhydrous dichloromethane was added into pyrazole (110 mmol) or 3,5-dimethylpyrazole (110 mmol). The mixture was stirred and refluxed for 4 h. After cooling, the solvent

was evaporated off under reduced pressure, and the solid was recrystallized from ethanol to obtain the title compounds **3a-3k** and **4a-4k**.

4.1.3.1. [2-(4-chlorophenyl)-1,3-oxazol-4-yl](1H-pyrazol-1-yl)methanone (**3a**):

Compound **3a** was obtained (82%) as a white solid. mp: 156-157 °C; ¹H NMR (600 MHz, CDCl₃) δ 6.55 (dd, *J* = 2.9, 1.5 Hz, 1H), 7.48-7.51 (m, 2H), 7.82 (dd, *J* = 1.4, 0.6 Hz, 1H), 8.12-8.15 (m, 2H), 8.52 (dd, *J* = 2.9, 0.7 Hz, 1H), 9.10 (s, 1H); ¹³C NMR (150 MHz, CDCl₃) δ 109.80, 124.67, 128.34, 129.24, 129.88, 133.59, 137.61, 144.56, 147.99, 157.78, 161.07; ESIMS(*m/z*): 274.3 [M + H]⁺. Anal. Calcd. (%) for C₁₃H₈ClN₃O₂: C, 57.21; H, 3.10; N, 15.11. Found: C, 57.05; H, 2.95; N, 15.35.

4.1.3.2. [2-(2-hydroxyphenyl)-1,3-oxazol-4-yl](1H-pyrazol-1-yl)methanone (**3b**):

Compound **3b** was obtained (80%) as a yellow solid. mp: 175-176 °C; ¹H NMR (600 MHz, DMSO-*d*₆) δ 6.56 (dd, *J* = 2.8, 1.5 Hz, 1H), 7.00 (ddd, *J* = 8.0, 7.3, 1.1 Hz, 1H), 7.14 (dd, *J* = 8.4, 0.8 Hz, 1H), 10.79 (s, 1H), 7.42-7.46 (m, 1H), 7.83 (dd, *J* = 1.4, 0.6 Hz, 1H), 7.90 (dd, *J* = 7.9, 1.6 Hz, 1H), 8.47 (dd, *J* = 2.9, 0.6 Hz, 1H), 9.08 (s, 1H); ¹³C NMR (150 MHz, DMSO-*d*₆) δ 109.96, 109.98, 117.61, 119.61, 126.36, 129.73, 131.91, 133.40, 144.66, 146.55, 156.93, 157.70, 161.51; ESIMS(*m/z*): 256.1 [M + H]⁺. Anal. Calcd. (%) for C₁₃H₉N₃O₃: C, 60.99; H, 3.47; N, 16.58. Found: C, 61.18; H, 3.55; N, 16.46.

4.1.3.3. [2-(4-methoxyphenyl)-1,3-oxazol-4-yl](1H-pyrazol-1-yl)methanone (**3c**):

Compound **3c** was obtained (91%) as a white solid. mp: 171-172 °C; ¹H NMR (600 MHz, CDCl₃) δ 3.87 (s, 3H), 6.52 (dd, *J* = 2.8, 1.4 Hz, 1H), 6.99 (d, *J* = 8.9 Hz, 2H), 7.80 (s, 1H), 8.11 (d, *J* = 8.9 Hz, 2H), 8.50 (d, *J* = 2.8 Hz, 1H), 9.02 (s, 1H); ¹³C NMR (150 MHz, CDCl₃) δ 55.44, 109.63, 114.28, 118.89, 128.83, 129.88, 133.32, 144.42, 147.52, 158.04, 162.07, 162.09; ESIMS(*m/z*): 270.1 [M + H]⁺. Anal. Calcd. (%) for C₁₃H₉N₃O₃: C, 62.68; H, 4.37; N, 15.41. Found: C, 62.45; H, 4.12; N, 15.61.

4.1.3.4. [2-(4-methylphenyl)-1,3-oxazol-4-yl](1H-pyrazol-1-yl)methanone (**3d**):

Compound **3d** was obtained (90%) as a white solid. mp: 91-92 °C; ¹H NMR (600 MHz, CDCl₃) δ 2.42 (s, 3H), 6.53 (dd, *J* = 2.8, 1.5 Hz, 1H), 7.30 (d, *J* = 7.9 Hz, 2H), 7.80 (d, *J* = 0.8 Hz, 1H), 8.07 (d, *J* = 8.2 Hz, 2H), 8.51 (dd, *J* = 2.8, 0.5 Hz, 1H), 9.06 (s, 1H); ¹³C NMR (150 MHz, CDCl₃) δ 21.60, 109.64,

123.51, 127.04, 129.57, 133.38, 129.89, 141.79, 144.43, 147.68, 157.98 162.22; ESIMS(m/z): 254.1 [M + H]⁺. Anal. Calcd. (%) for C₁₄H₁₁N₃O₂: C, 66.24; H, 4.61; N, 16.32. Found: C, 66.40; H, 4.38; N, 16.59.

4.1.3.5. [2-(3-methoxyphenyl)-1,3-oxazol-4-yl](1H-pyrazol-1-yl)methanone (3e):

Compound **3e** was obtained (87%) as a white solid. mp: 134-135 °C; ¹H NMR (600 MHz, CDCl₃) δ 3.91 (s, 3H), 6.54 (dd, $J = 2.8, 1.5$ Hz, 1H), 7.07 (ddd, $J = 8.3, 2.6, 0.9$ Hz, 1H), 7.41 (t, $J = 8.0$ Hz, 1H), 7.72 (dd, $J = 2.5, 1.6$ Hz, 1H), 7.74-7.77 (m, 1H), 7.81 (d, $J = 0.8$ Hz, 1H), 8.51 (dd, $J = 2.8, 0.5$ Hz, 1H), 9.09 (s, 1H); ¹³C NMR (150 MHz, CDCl₃) δ 55.62, 109.73, 111.50, 118.17, 119.50, 127.38, 129.90, 129.97, 133.47, 144.51, 147.95, 157.95, 159.95, 161.92; ESIMS(m/z): 270.1 [M + H]⁺. Anal. Calcd. (%) for C₁₃H₉N₃O₃: C, 62.68; H, 4.37; N, 15.41. Found: C, 62.45; H, 4.12; N, 15.61.

4.1.3.6. (2-phenyl-1,3-oxazol-4-yl)(1H-pyrazol-1-yl)methanone (3f):

Compound **3f** was obtained (89%) as a white solid. mp: 139-140 °C; ¹H NMR (600 MHz, CDCl₃) δ 6.53 (dd, $J = 2.8, 1.5$ Hz, 1H), 7.80 (d, $J = 0.8$ Hz, 1H), 7.48-7.52 (m, 3H), 8.16-8.19 (m, 2H), 8.50 (d, $J = 2.8$ Hz, 1H), 9.08 (s, 1H); ¹³C NMR (150 MHz, CDCl₃) δ 109.70, 126.18, 127.04, 128.84, 129.86, 131.30, 133.46, 144.48, 147.91, 157.88, 161.95; ESIMS(m/z): 240.1 [M + H]⁺. Anal. Calcd. (%) for C₁₃H₉N₃O₂: C, 65.42; H, 3.54; N, 17.81. Found: C, 65.27; H, 3.79; N, 17.56.

4.1.3.7. [2-(4-bromophenyl)-1,3-oxazol-4-yl](1H-pyrazol-1-yl)methanone (3g):

Compound **3g** was obtained (87%) as a yellow solid. mp: 167-168 °C; ¹H NMR (600 MHz, CDCl₃) δ 6.54 (dd, $J = 2.7, 1.4$ Hz, 1H), 7.64 (d, $J = 8.5$ Hz, 2H), 7.81 (s, 1H), 8.05 (d, $J = 8.5$ Hz, 2H), 8.50 (d, $J = 2.8$ Hz, 1H), 9.08 (s, 1H); ¹³C NMR (150 MHz, CDCl₃) δ 109.79, 125.10, 126.03, 128.48, 129.86, 132.19, 133.61, 144.55, 148.00, 157.74, 161.13; ESIMS(m/z): 318.1 [M + H]⁺. Anal. Calcd. (%) for C₁₃H₈BrN₃O₂: C, 49.25; H, 2.37; N, 13.07. Found: C, 49.08; H, 2.53; N, 13.21.

4.1.3.8. [2-(4-fluorophenyl)-1,3-oxazol-4-yl](1H-pyrazol-1-yl)methanone (3h):

Compound **3h** was obtained (90%) as a white solid. mp: 157-158 °C; ¹H NMR (600 MHz, CDCl₃) δ 6.54 (dd, $J = 2.7, 1.4$ Hz, 1H), 7.21-7.17 (m, 2H), 7.81 (s, 1H), 8.16-8.21 (m, 2H), 8.50 (d, $J = 2.8$ Hz, 1H), 9.07 (s, 1H); ¹³C NMR (150 MHz, CDCl₃) δ 109.76, 116.15 (d, ² $J_{C-F} = 22.2$ Hz), 122.57 (d, ⁴ $J_{C-F} =$

3.1 Hz), 129.32 (d, $^3J_{\text{C-F}} = 8.8$ Hz), 129.89, 133.51, 144.53, 147.89, 157.86, 161.16, 164.65 (d, $^1J_{\text{C-F}} = 252.6$ Hz); ESIMS(m/z): 258.2 $[\text{M} + \text{H}]^+$. Anal. Calcd. (%) for $\text{C}_{13}\text{H}_8\text{FN}_3\text{O}_2$: C, 60.92; H, 2.98; N, 16.11. Found: C, 60.70; H, 3.13; N, 16.34.

4.1.3.9. [2-(3-hydroxyphenyl)-1,3-oxazol-4-yl](1H-pyrazol-1-yl)methanone (3i):

Compound **3i** was obtained (80%) as a white solid. mp: 199-200 °C; ^1H NMR (600 MHz, $\text{DMSO-}d_6$) δ 6.74 (dd, $J = 2.8, 1.5$ Hz, 1H), 7.01 (ddd, $J = 8.1, 2.5, 0.9$ Hz, 1H), 7.40 (t, $J = 7.9$ Hz, 1H), 7.48-7.50 (m, 1H), 7.50-7.52 (m, 1H), 8.04 (d, $J = 0.9$ Hz, 1H), 8.65 (dd, $J = 2.8, 0.5$ Hz, 1H), 9.27 (s, 1H), 9.96 (s, 1H); ^{13}C NMR (150 MHz, $\text{DMSO-}d_6$) δ 110.83, 113.35, 117.64, 119.16, 127.27, 130.68, 130.99, 133.05, 145.56, 149.20, 157.69, 158.37, 161.36; ESIMS(m/z): 256.1 $[\text{M} + \text{H}]^+$. Anal. Calcd. (%) for $\text{C}_{13}\text{H}_9\text{N}_3\text{O}_3$: C, 59.92; H, 3.78; N, 16.24. Found: C, 61.18; H, 3.55; N, 16.46.

4.1.3.10. [2-(4-hydroxyphenyl)-1,3-oxazol-4-yl](1H-pyrazol-1-yl)methanone (3j):

Compound **3j** was obtained (89%) as a white solid. mp: 209-210 °C; ^1H NMR (600 MHz, $\text{DMSO-}d_6$) δ 6.73 (dd, $J = 2.8, 1.5$ Hz, 1H), 6.97-6.94 (m, 2H), 10.26 (s, 1H), 7.90-7.93 (m, 2H), 8.02 (d, $J = 0.9$ Hz, 1H), 8.64 (d, $J = 2.8$ Hz, 1H), 9.20 (s, 1H); ^{13}C NMR (150 MHz, $\text{DMSO-}d_6$) δ 110.77, 116.52, 117.14, 128.92, 130.70, 132.89, 145.51, 148.58, 157.81, 160.95, 161.81; ESIMS(m/z): 256.1 $[\text{M} + \text{H}]^+$. Anal. Calcd. (%) for $\text{C}_{13}\text{H}_9\text{N}_3\text{O}_3$: C, 61.31; H, 3.67; N, 16.71. Found: C, 61.18; H, 3.55; N, 16.46.

4.1.3.11. [2-(3-fluorophenyl)-1,3-oxazol-4-yl](1H-pyrazol-1-yl)methanone (3k):

Compound **3k** was obtained (92%) as a white solid. mp: 146-147 °C; ^1H NMR (600 MHz, CDCl_3) δ 6.54 (dd, $J = 2.8, 1.5$ Hz, 1H), 7.22 (tdd, $J = 8.3, 2.5, 0.6$ Hz, 1H), 7.48 (td, $J = 8.0, 5.6$ Hz, 1H), 7.81 (d, $J = 0.6$ Hz, 1H), 7.88 (ddd, $J = 9.4, 2.3, 1.7$ Hz, 1H), 7.98 (d, $J = 7.8$ Hz, 1H), 8.50 (d, $J = 2.8$ Hz, 1H), 9.10 (s, 1H); ^{13}C NMR (150 MHz, CDCl_3) δ 109.79, 114.16 (d, $^2J_{\text{C-F}} = 24.2$ Hz), 118.38 (d, $^2J_{\text{C-F}} = 21.3$ Hz), 122.87 (d, $^4J_{\text{C-F}} = 3.0$ Hz), 128.27 (d, $^3J_{\text{C-F}} = 9.1$ Hz), 129.93, 130.69 (d, $^3J_{\text{C-F}} = 8.2$ Hz), 133.77, 144.56, 148.11, 157.74, 160.89 (d, $^4J_{\text{C-F}} = 3.3$ Hz), 162.99 (d, $^1J_{\text{C-F}} = 247.2$ Hz); ESIMS(m/z): 258.1 $[\text{M} + \text{H}]^+$. Anal. Calcd. (%) for $\text{C}_{13}\text{H}_8\text{FN}_3\text{O}_2$: C, 60.88; H, 3.01; N, 16.10. Found: C, 60.70; H, 3.13; N, 16.34.

4.1.3.12. [2-(4-chlorophenyl)-1,3-oxazol-4-yl](3,5-dimethyl-1H-pyrazol-1-yl)methanone (4a):

Compound **4a** was obtained (82%) as a white solid. mp: 158-159 °C; ¹H NMR (600 MHz, CDCl₃) δ 2.30 (s, 3H), 2.65 (s, 3H), 6.05 (s, 1H), 7.44-7.50 (m, 2H), 8.08-8.13 (m, 2H), 8.97 (s, 1H); ¹³C NMR (150 MHz, CDCl₃) δ 13.92, 14.52, 111.30, 124.95, 128.22, 129.17, 134.61, 137.32, 145.48, 147.20, 152.83, 159.31, 160.59; ESIMS(*m/z*): 302.3 [M + H]⁺. Anal. Calcd. (%) for C₁₅H₁₂ClN₃O₂: C, 59.92; H, 3.86; N, 14.14. Found: C, 59.71; H, 4.01; N, 13.93.

4.1.3.12. [2-(2-hydroxyphenyl)-1,3-oxazol-4-yl](3,5-dimethyl-1H-pyrazol-1-yl)methanone (4b):

Compound **4b** was obtained (82%) as a white solid. mp: 177-178 °C; ¹H NMR (600 MHz, DMSO-*d*₆) δ 2.28 (s, 3H), 2.57 (s, 3H), 6.32 (s, 1H), 7.04-7.07 (m, 1H), 7.11 (d, *J* = 8.3 Hz, 1H), 7.50-7.46 (m, 1H), 7.88 (dd, *J* = 7.8, 1.5 Hz, 1H), 9.25 (s, 1H), 10.82 (s, 1H); ¹³C NMR (150 MHz, DMSO-*d*₆) δ 14.02, 14.48, 111.04, 112.15, 117.56, 120.34, 127.64, 132.70, 133.74, 145.01, 147.79, 153.12, 157.02, 158.58, 160.68; ESIMS(*m/z*): 284.2 [M + H]⁺. Anal. Calcd. (%) for C₁₅H₁₃N₃O₃: C, 63.41; H, 4.82; N, 15.03. Found: C, 63.60; H, 4.63; N, 14.83.

4.1.3.14. [2-(4-methoxyphenyl)-1,3-oxazol-4-yl](3,5-dimethyl-1H-pyrazol-1-yl)methanone (4c):

Compound **4c** was obtained (92%) as a white solid. mp: 125-126 °C; ¹H NMR (600 MHz, CDCl₃) δ 2.30 (s, 3H), 2.65 (s, 3H), 3.87 (s, 3H), 6.04 (s, 1H), 6.97-7.00 (m, 2H), 8.09-8.12 (m, 2H), 8.92 (s, 1H); ¹³C NMR (150 MHz, CDCl₃) δ 13.91, 14.53, 55.41, 111.15, 114.21, 119.21, 128.68, 134.33, 145.41, 146.70, 152.63, 159.61, 161.59, 161.89; ESIMS(*m/z*): 298.1 [M + H]⁺. Anal. Calcd. (%) for C₁₆H₁₅N₃O₃: C, 64.85; H, 4.89; N, 14.35. Found: C, 64.64; H, 5.09; N, 14.13.

4.1.3.15. [2-(4-methylphenyl)-1,3-oxazol-4-yl](3,5-dimethyl-1H-pyrazol-1-yl)methanone (4d):

Compound **4d** was obtained (85%) as a white solid. mp: 125-126 °C; ¹H NMR (600 MHz, CDCl₃) δ 2.30 (s, 3H), 2.41 (s, 3H), 2.65 (s, 3H), 6.04 (s, 1H), 7.28 (d, *J* = 8.0 Hz, 2H), 8.05 (d, *J* = 8.2 Hz, 2H), 8.94 (s, 1H); ¹³C NMR (150 MHz, CDCl₃) δ 13.91, 14.53, 21.57, 111.18, 123.79, 126.92, 129.51, 134.38, 141.48, 145.42, 146.88, 152.67, 159.54, 161.73; ESIMS(*m/z*): 282.1 [M + H]⁺. Anal. Calcd. (%) for C₁₆H₁₅N₃O₂: C, 68.18; H, 5.64; N, 14.69. Found: C, 68.31; H, 5.37; N, 14.94.

4.1.3.16. [2-(3-methoxyphenyl)-1,3-oxazol-4-yl](3,5-dimethyl-1H-pyrazol-1-yl)methanone (4e):

Compound **4e** was obtained (92%) as a white solid. mp: 133-134 °C; ^1H NMR (600 MHz, CDCl_3) δ 2.30 (s, 3H), 2.65 (s, 3H), 3.89 (s, 3H), 6.04 (s, 1H), 7.04 (dd, $J = 8.0, 2.2$ Hz, 1H), 7.38 (t, $J = 7.9$ Hz, 1H), 7.75-7.69 (m, 2H), 8.97 (s, 1H); ^{13}C NMR (150 MHz, CDCl_3) δ 13.89, 14.51, 55.55, 111.24, 111.31, 117.94, 119.33, 127.63, 129.87, 134.45, 145.43, 147.17, 152.74, 159.46, 159.58, 161.39; ESIMS(m/z): 298.1 $[\text{M} + \text{H}]^+$. Anal. Calcd. (%) for $\text{C}_{16}\text{H}_{15}\text{N}_3\text{O}_3$: C, 64.47; H, 5.31; N, 14.29. Found: C, 64.64; H, 5.09; N, 14.13.

4.1.3.17. (2-phenyl-1,3-oxazol-4-yl)(3,5-dimethyl-1H-pyrazol-1-yl)methanone (4f):

Compound **4f** was obtained (82%) as a white solid. mp: 125-126 °C; MW: 267.10; ^1H NMR (600 MHz, CDCl_3) δ 2.29 (s, 3H), 2.65 (s, 3H), 6.04 (s, 1H), 7.46-7.50 (m, 3H), 8.15-8.18 (m, 2H), 8.97 (s, 1H); ^{13}C NMR (150 MHz, CDCl_3) δ 13.90, 14.52, 111.21, 126.45, 126.92, 128.77, 131.04, 134.47, 145.40, 147.11, 152.70, 159.43, 161.47; ESIMS(m/z): 268.1 $[\text{M} + \text{H}]^+$. Anal. Calcd. (%) for $\text{C}_{15}\text{H}_{13}\text{N}_3\text{O}_2$: C, 67.66; H, 5.10; N, 15.48. Found: C, 67.40; H, 4.90; N, 15.72.

4.1.3.18. [2-(4-bromophenyl)-1,3-oxazol-4-yl](3,5-dimethyl-1H-pyrazol-1-yl)methanone (4g):

Compound **4g** was obtained (85%) as a white solid. mp: 167-168 °C; ^1H NMR (600 MHz, CDCl_3) δ 2.30 (s, 3H), 2.65 (s, 3H), 6.05 (s, 1H), 7.61-7.65 (m, 2H), 8.02-8.05 (m, 2H), 8.97 (s, 1H); ^{13}C NMR (150 MHz, CDCl_3) δ 13.92, 14.52, 111.31, 125.38, 125.74, 128.38, 132.14, 134.64, 145.48, 147.23, 152.83, 159.29, 160.65; ESIMS(m/z): 347.1 $[\text{M} + \text{H}]^+$. Anal. Calcd. (%) for $\text{C}_{15}\text{H}_{12}\text{BrN}_3\text{O}_2$: C, 52.31; H, 3.24; N, 12.31. Found: C, 52.04; H, 3.49; N, 12.14.

4.1.3.19. [2-(4-fluorophenyl)-1,3-oxazol-4-yl](3,5-dimethyl-1H-pyrazol-1-yl)methanone (4h):

Compound **4h** was obtained (85%) as a white solid. mp: 131-132 °C; ^1H NMR (600 MHz, CDCl_3) δ 2.30 (s, 3H), 2.65 (s, 3H), 6.05 (s, 1H), 7.14-7.19 (m, 2H), 8.14-8.18 (m, 2H), 8.96 (s, 1H); ^{13}C NMR (150 MHz, CDCl_3) δ 13.91, 14.52, 111.28, 116.06 (d, $^2J_{\text{C-F}} = 22.2$ Hz), 122.84 (d, $^4J_{\text{C-F}} = 3.2$ Hz), 129.17 (d, $^3J_{\text{C-F}} = 8.8$ Hz), 134.52, 145.47, 147.10, 152.80, 159.40, 160.68, 164.50 (d, $^1J_{\text{C-F}} = 251.9$ Hz); ESIMS(m/z): 286.1 $[\text{M} + \text{H}]^+$. Anal. Calcd. (%) for $\text{C}_{15}\text{H}_{12}\text{FN}_3\text{O}_2$: C, 62.97; H, 4.08; N, 14.92. Found: C, 63.15; H, 4.24; N, 14.73.

4.1.3.20. [2-(3-hydroxyphenyl)-1,3-oxazol-4-yl](3,5-dimethyl-1H-pyrazol-1-yl)methanone (4i):

Compound **4i** was obtained (92%) as a yellow solid. mp: 193-194 °C; ^1H NMR (600 MHz, DMSO- d_6) δ 2.27 (s, 3H), 2.56 (s, 3H), 6.29 (s, 1H), 6.98 (ddd, $J = 8.1, 2.3, 0.7$ Hz, 1H), 7.39 (t, $J = 7.9$ Hz, 1H), 7.45-7.50 (m, 2H), 9.16 (s, 1H), 9.93 (s, 1H); ^{13}C NMR (150 MHz, DMSO- d_6) δ 14.00, 14.53, 111.97, 113.25, 117.54, 119.00, 127.49, 130.98, 134.03, 144.89, 148.63, 152.80, 158.37, 159.11, 160.91; ESIMS(m/z): 284.2 $[\text{M} + \text{H}]^+$. Anal. Calcd. (%) for $\text{C}_{15}\text{H}_{13}\text{N}_3\text{O}_3$: C, 63.81; H, 4.79; N, 14.58. Found: C, 63.60; H, 4.63; N, 14.83.

4.1.3.21. [2-(4-hydroxyphenyl)-1,3-oxazol-4-yl](3,5-dimethyl-1H-pyrazol-1-yl)methanone (**4j**):

Compound **4j** was obtained (91%) as a yellow solid. mp: 207-208 °C; ^1H NMR (600 MHz, DMSO- d_6) δ 2.26 (s, 3H), 2.56 (s, 3H), 6.29 (s, 1H), 6.93-6.96 (m, 2H), 7.87-7.90 (m, 2H), 9.09 (s, 1H), 10.22 (s, 1H); ^{13}C NMR (150 MHz, DMSO- d_6) δ 14.02, 14.55, 111.92, 116.50, 117.40, 128.79, 133.86, 144.85, 148.00, 152.71, 159.29, 160.81, 161.36; ESIMS(m/z): 284.1 $[\text{M} + \text{H}]^+$. Anal. Calcd. (%) for $\text{C}_{15}\text{H}_{13}\text{N}_3\text{O}_3$: C, 63.79; H, 4.48; N, 14.61. Found: C, 63.60; H, 4.63; N, 14.83.

4.1.3.22. [2-(3-fluorophenyl)-1,3-oxazol-4-yl](3,5-dimethyl-1H-pyrazol-1-yl)methanone (**4k**):

Compound **4k** was obtained (88%) as a white solid. mp: 141-142 °C; ^1H NMR (600 MHz, CDCl_3) δ 2.30 (s, 3H), 2.65 (d, $J = 0.7$ Hz, 3H), 6.05 (s, 1H), 7.22 (ddd, $J = 10.7, 8.4, 0.7$ Hz, 1H), 7.25-7.29 (m, 1H), 7.50-7.46 (m, 1H), 8.21 (td, $J = 7.6, 1.7$ Hz, 1H), 9.03 (s, 1H); ^{13}C NMR (150 MHz, CDCl_3) δ 13.88, 14.48, 111.26, 114.81 (d, $^3J_{\text{C-F}} = 11.0$ Hz), 116.82 (d, $^2J_{\text{C-F}} = 21.2$ Hz), 124.39 (d, $^4J_{\text{C-F}} = 3.7$ Hz), 130.33, 132.77 (d, $^3J_{\text{C-F}} = 8.4$ Hz), 134.29, 145.42, 147.42, 152.77, 158.31 (d, $^4J_{\text{C-F}} = 3.8$ Hz), 159.25, 160.26 (d, $^1J_{\text{C-F}} = 257.9$ Hz); ESIMS(m/z): 286.1 $[\text{M} + \text{H}]^+$. Anal. Calcd. (%) for $\text{C}_{15}\text{H}_{12}\text{FN}_3\text{O}_2$: C, 63.37; H, 4.01; N, 14.88. Found: C, 63.15; H, 4.24; N, 14.73.

4.2. Bioassay

4.2.1. Assay of human PDE4 activity

Phosphodiesterase type 4 isozyme (PDE4) was isolated with the modified method.^{19,20} The enzyme was prepared from U937 cells which was derived from human monocytes, and was stored at -20 °C after preparation. Measurement of PDE4 activity was performed using this stored enzyme after it was diluted with distilled water containing bovine serum albumin. The substrate solution was prepared by adding

[³H]-cAMP (300,000 dpm (5000 Bq)/assay) and 100 μmol/L cAMP solution to 100 mmol/L Tris-HCl (pH 8.0) containing 5 mmol/L ethylene glycol-bis (β-aminoethyl ether) and *O,O'*-bis(2-aminoethyl)ethyleneglycol-*N,N,N',N'*-tetraacetic acid. The substrate solution was mixed with the enzyme solution containing a test compound dissolved in DMSO, and incubation was done for 30 min at 30 °C. Assays were performed in duplicate at different concentrations of each test compound.

4.2.2. Assay of TNF-α release.

The blood is mixed with saline at a ratio of 1:1, and the peripheral blood mononuclear cells (PBMCs) were isolated from buffy coats using Lymphoprep tubes. The PBMCs were suspended in RPMI 1640 with 0.5% human serum albumin, pen/ strep, and 2 mM L-glutamine at 5×10^5 cells/mL. The cells were pre-incubated with the test compounds in 96-well plates for 30 min and stimulated for 18 h with 1 mg/mL lipopolysaccharide. TNF-α concentration in the supernatants was measured by homogeneous time-resolved fluorescence resonance (TR-FRET). The assay is quantified by measuring fluorescence at 665 nm (proportional to TNF-α concentration) and 620 nm (control). Results are expressed as IC₅₀ values (μM).

4.2.3. LPS induced sepsis for measurement of TNF-α inhibition in mice

The LPS induced sepsis model in mice was evaluated following the literature.²¹ Female *Swiss albino* mice were selected according to the body weights, which were equivalent within each group. The mice were fasted for 20 h with free access to water and dosed for oral administration (po) with the test compounds suspended in vehicle containing 0.5% Tween 80 in 0.25% sodium salt of carboxymethylcellulose. The control mice were performed the vehicle alone. After 30 min of oral dosing, the mice were injected into intraperitoneal cavity with 500 μg of lipopolysaccharide (*Escherichia coli*, LPS: B4 from Sigma) in phosphate buffer. Then the mice were bled *via* retro-orbital sinus puncture after 90 min of LPS administration. Serum samples were collected by centrifuging the blood samples at 4000 rpm for 20 min, which were stored overnight at 4 °C. Immediately, the serum samples were checked for TNF-α levels using commercial mouse TNF-α ELISA kit (Amersham Biosciences) and assay was carried out following the manufacturer instruction.

4.2.4. LPS induced neutrophilia model for asthma and COPD

LPS induced neutrophilia in *Sprague Dawley* rats was assessed according to the protocol described.²² Male *Sprague Dawley* rats were acclimatized to laboratory conditions for one week prior to the experiment. According to the body weight, the rats were distributed to various groups randomly. Except normal group, all the rats were exposed to 100 µg/mL lipopolysaccharide (*Escherichia coli*, LPS: B4 from Sigma) for 40 min. The rats were dosed for oral administration (po) with the test compounds suspended in the vehicle containing 0.25% sodium salt of carboxymethylcellulose before half an hour of LPS exposure. Bronchoalveolar lavage (BAL) was performed 6 h after LPS exposure, total cell count and DLC (differential leukocyte count) were checked and compared with control.

4.4. Molecular docking

Molecular docking was performed on Surflex-Dock module of Sybyl 8.0.^{14,23,24} Crystal structure of PDE4B (PDB ID: 1XMY) obtained from Protein Data Bank was used as the receptor for molecular docking study. The 3D structure of compounds **3c** and **4c** was drawn and optimized with SYBYL package. The docking procedure was started with the protomol generation, which was created using a ligand-based approach (native ligand for PDE4B structure). Proto threshold was set to 0.5 and proto bloat was kept at 0 as a default parameter. For docking, max conformation and max rotation values were 20 and 100, respectively. Pre-dock and post-dock energy minimization methods were also applied. Docking results were compared by the total score values. The pose with the higher total-score value was considered as the best one. After the end of molecular docking, the interactions of the docked domain with ligand were analyzed.

Acknowledgments

We acknowledge the financial supports from the Special Fund for the National Natural Science Foundation of China (31570122), the National Key Project for Basic Research (973 Program, 2015CB150600), the Pearl River S&T Nova Program of Guangzhou (201506010029), the Research and Construction of Public Service Ability (2014A020210019 and 2016A020217014), the Opening

Foundation of the Key Laboratory of Green Pesticide and Agricultural Bioengineering, Ministry of Education, Guizhou University (2015GDGP0101).

References and notes

1. Jeon, Y. H.; Heo, Y. S.; Kim, C. M.; Hyun, Y. L.; Lee, T. G.; Ro, S.; Cho, J. M. *Cell. Mol. Life Sci.* **2005**, 62, 1198.
2. Manallack, D. T.; Hughes, R. A.; Thompson, P. E. *J. Med. Chem.* **2005**, 48, 3449.
3. Beavo, J. A.; Reifsnnyder, D. H. *Trends Pharmacol. Sci.* **1990**, 11, 150.
4. Tasken, K.; Aandahl, E. M. *Physiol. Rev.* **2004**, 84, 137.
5. Kodimuthali, A.; Jabarisi, S. L.; Pal, M. *J. Med. Chem.* **2008**, 51, 5471.
6. Huang, Z.; Mancici, J. A. *Curr. Med. Chem.* **2006**, 13, 3253.
7. Houslay, M.; Schafer, P.; Zhang, K. Y. *J. Drug Discovery Today.* **2005**, 10, 1503.
8. Beavo, J. A.; Reifsnnyder, D. H. *Trends Pharmacol. Sci.* **1990**, 11, 150.
9. Zhu, J.; Mix, E.; Winblad, B. *CNS Drug Rev.* **2001**, 7, 387.
10. Zhou, Z. Z.; Cheng, Y. F.; Zou, Z. Q.; Ge, B. C.; Yu, H.; Huang, C.; Wang, H. T.; Yang, X. M.; Xu, J. P. *ACS Chem. Neurosci.* **2016**, DOI:10.1021/acchemneuro.6b00271.
11. Zhou, Z. Z.; Ge, B. C.; Zhong, Q. P.; Huang, C.; Cheng, Y. F.; Yang, X. M.; Wang, H. T.; Xu, J. P. *Eur. J. Med. Chem.* **2016**, 124, 372.
12. Norman, P. *Expert Opin. Ther. Pat.* **1998**, 8, 771.
13. Losco, P. E.; Evans, E. W.; Barat, S. A.; Blackshear, P. E.; Reyderman, L.; Fine, J. S.; Bober, L. A.; Anthes, J. C.; Mirro, E. J.; Cuss, F. M. *Toxicol. Pathol.* **2004**, 32, 295.
14. Song, G. P.; Zhao, D. S.; Hu, D. K.; Li, Y. S.; Jin, H. W.; Cui, Z. N. *Bioorg. Med. Chem. Lett.* **2015**, 25, 4610.
15. Zhou, Z. Z.; Ge, B. C.; Chen, Y. F.; Shi, X. D.; Yang, X. M.; Xu, J. P. *Bioorg. Med. Chem.* **2015**, 23, 7332.

16. Kuang, R.; Shue, H. J.; Blythin, D. J.; Shih, N. Y.; Gu, D.; Chen, X.; Schwerdt, J.; Lin, L.; Ting, P. C.; Zhu, X.; Aslanian, R.; Xiao, L.; Prelusky, D.; Wu, P.; Zhang, J.; Zhang, X.; Celly, C. S.; Minnicozzi, M.; Billah, M.; Wang, P. *Bioorg. Med. Chem. Lett.* **2007**, *17*, 5150.
17. Kuang, R.; Shue, H. J.; Xiao, L.; Blythin, D. J.; Shih, N. Y.; Chen, X.; Gu, D.; Schwerdt, J.; Ling, L.; Ting, P. C.; Cao, J.; Aslanian, R.; Piwinski, J. J.; Prelusky, D.; Wu, P.; Zhang, J.; Zhang, X.; Celly, C. S.; Billah, M.; Wang, P. *Bioorg. Med. Chem. Lett.* **2012**, *22*, 2594.
18. Ting, P. C.; Lee, J. F.; Kuang, R.; Cao, J.; Gu, D.; Huang, Y.; Liu, Z.; Aslanian, R. G.; Feng, K. I.; Prelusky, D.; Lamca, J.; House, A.; Phillips, J. E.; Wang, P.; Wu, P.; Lundell, D.; Chapman, R. W.; Celly, C. S. *Bioorg. Med. Chem. Lett.* **2013**, *23*, 5528.
19. Li, Y. S.; Tian, H.; Zhao, D. S.; Hu, D. K.; Liu, X. Y.; Jin, H. W.; Song, G. P.; Cui, Z. N. *Bioorg. Med. Chem. Lett.* **2016**, *26*, 3632.
20. Ochiai, H.; Odagaki, Y.; Ohtani, T.; Ishida, A.; Kusumi, K.; Kishikawa, K.; Yamamoto, S.; Takeda, H.; Obata, T.; Kobayashi, K.; Nakai, H.; Toda, M. *Bioorg. Med. Chem.* **2004**, *12*, 5063.
21. Sekut, L.; Menius, J. A., Jr.; Brackeen, M. F.; Connolly, K. M. *J. Lab. Clin. Med.* 1994, *124*, 813.
22. Spond, J.; Billah, M. M.; Chapman, R. W.; Egan, R. W.; Hey, J. A.; House, A.; Kreutner, W.; Minnicozzi, M. *Pulm. Pharmacol. Ther.* 2004, *17*, 133.
23. Morris, G. M.; Goodsell, D. S.; Halliday, R. S.; Huey, R.; Hart, W. E. *J. Comput. Chem.* **1998**, *19*, 1639.
24. Song, G. P.; Li, S. M.; Si, H. Z.; Li, Y. B.; Li, Y. S.; Fan, J. H.; Liang, Q. Q.; He, H. B.; Ye, H. M.; Cui, Z. N. *RSC Adv.* **2015**, *5*, 36092.

Figure captions

Figure 1. The designed strategy for the title compounds.

Figure 2. Model of PDE4 and docking of compounds **3c** and **4c**. (A, B) The entire PDE4B structure (N-terminal domain, a catalytic domain and a C-terminal domain) bound to **3c**. (C, D) The catalytic domain bound to **3c**. (E, F) The catalytic domain bound to **4c**. (G, H) The catalytic domain bound to **4c** overlaid with rolipram (orange).

Scheme 1. The synthetic route of the title compounds **3a-3k** and **4a-4k**.

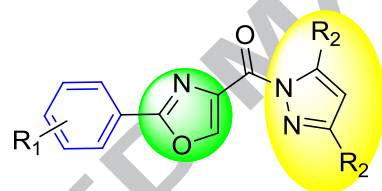
Table 1 Impact on enzymatic potency (PDE4B) and inhibition of TNF- α release from human blood mononuclear cells stimulated with lipopolysaccharide

Table 2 LPS induced TNF- α in SA mice and neutrophil influx in BALF of SD rats

Design, Synthesis and Biological Evaluation of 2,4-Disubstituted Oxazole Derivatives as Potential PDE4 Inhibitors

Ya-Sheng Li ^{a,#}, De-Kun Hu ^{a,#}, Dong-Sheng Zhao ^{c,#}, Xing-Yu Liu ^a,

Hong-Wei Jin ^d, Gao-Peng Song ^{b,*}, Zi-Ning Cui ^{a,*}, Lian-Hui Zhang ^a



4c ($R_1 = 4\text{-OCH}_3$, $R_2 = \text{CH}_3$)

$\text{IC}_{50} = 1.6 \mu\text{M}$ (PDE4B)

$\text{IC}_{50} = 10.3 \mu\text{M}$ ($\text{TNF-}\alpha$)

